Impaired Long-Term Potentiation, Spatial Learning, and Hippocampal Development in *fyn* Mutant Mice

Seth G. N. Grant, Thomas J. O'Dell, Kevin A. Karl, Paul L. Stein, Philippe Soriano, Eric R. Kandel

Mice with mutations in four nonreceptor tyrosine kinase genes, *fyn*, *src*, *yes*, and *abl*, were used to study the role of these kinases in long-term potentiation (LTP) and in the relation of LTP to spatial learning and memory. All four kinases were expressed in the hippocampus. Mutations in *src*, *yes*, and *abl* did not interfere with either the induction or the maintenance of LTP. However, in *fyn* mutants, LTP was blunted even though synaptic transmission and two short-term forms of synaptic plasticity, paired-pulse facilitation and post-tetanic potentiation, were normal. In parallel with the blunting of LTP, *fyn* mutants showed impaired spatial learning, consistent with a functional link between LTP and learning. Although *fyn* is expressed at mature synapses, its lack of expression during development resulted in an increased number of granule cells in the dentate gyrus and of pyramidal cells in the CA3 region. Thus, a common tyrosine kinase pathway may regulate the growth of neurons in the developing hippocampus and the strength of synaptic plasticity in the mature hippocampus.

The biological analysis of learning and memory requires the demonstration of a causal relation between molecular mechanisms in neurons of the brain implicated in a particular form of learning and the modification of behavior produced by the learning. In invertebrate animals with few neurons, it is possible to assign a role to the actions of specific genes and proteins in the synaptic plasticity of individual cells (or cell groupings) and to relate the plasticity to the modifications of behavior produced by learning in the whole animal (*1*). This relation is more difficult to demonstrate in mammals, particularly for complex forms of learning involving the hippocampus and neocortex. However, the ability to generate specific gene mutations in mice, by homologous recombination in embryonic stem (ES) cells, makes it possible to relate the actions of known genes to the physiology of specific cells in regions thought to be necessary for learning as well as to learned behavior in the whole animal.

In humans, the hippocampus has a central role in the long-term storage of explicit memories, which result in the conscious remembrance of places, people, and objects (*2*). These findings have been extended to monkeys, rats, and mice, where spatial and olfactory memories are sensitive to hippocampal damage (*2*, *3*). In addition to their importance in behavioral learning, the neurons of the hippocampus undergo several enduring forms of synaptic plasticity. In particular, the strength of excitatory synaptic connections can be enhanced for prolonged periods after a short burst of high-frequency synaptic activity, a process known as long-term potentiation (LTP) (*4*).

LTP in the hippocampus has been well studied in the synaptic connections formed between the Schaffer collateral and commissural axons of the pyramidal cells in the CA3 region and their target cells, the pyramidal cells of the CA1 region (*5*). The excitatory transmitter at these synapses is L-glutamate, which activates both NMDA (*N*-methyl-D-aspartate) and non-NMDA receptors on CA1 neurons (*6*). High-frequency synaptic activity induces LTP by depolarizing the postsynaptic cells sufficiently to cause activation of the NMDA receptor, which results in an increase in Ca^{2+} influx. Ca^{2+} influx into the postsynaptic cell activates a cascade of protein kinases, including both serine-threonine (*7*) and tyrosine kinases (*8*, *9*). This kinase cascade is thought to lead to the release of retrograde synaptic messengers, which seem to enhance transmitter release by acting on the terminals of the presynaptic neuron (*10*).

The inhibitors of tyrosine kinases block the induction of LTP without affecting normal synaptic transmission, post-tetanic potentiation (PTP), or several physiological responses mediated by serine-threonine kinases (*8*). However, the inhibitors used to investigate the role of tyrosine kinases in LTP lack the pharmacological specificity necessary to identify specific tyrosine kinases.

Tyrosine kinases fall into two structurally distinct categories: (i) membrane-spanning receptor tyrosine kinases that transduce signals from growth and neurotrophic factors and (ii) nonreceptor tyrosine kinases associated with the cytoplasmic side of the plasma membrane (*11*). The nonreceptor tyrosine kinases are often associated with and activated by various transmembrane signaling molecules including the PDGF receptor (*12*) and the T cell receptor (*13*). To facilitate identification of individual tyrosine kinases involved in LTP, we have examined mice with mutations in the *src*,

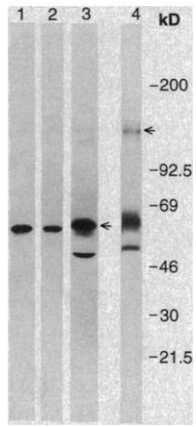

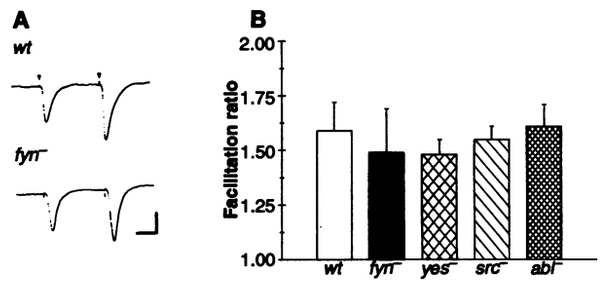

Fig. 1 (left). Expression of Fyn, Src, Yes, and Abl tyrosine kinases in mouse hippocampus by in vitro immune complex protein kinase assays. Proteins immunoprecipitated with antibodies specific to Fyn (lane 1), Src (lane 2), Yes (lane 3), and Abl (lane 4) were incubated with [γ^{32}P]ATP, separated by SDS–polyacrylamide gel electrophoresis, and KOH treated to reveal tyrosine phosphorylation. Film was exposed for 2 hours for Fyn, Src, and Yes and overnight for Abl (*44*). Arrows indicate Yes and Abl. **Fig. 2 (right)**. Paired-pulse facilitation in hippocampal slices from *fyn*$^-$ (n = 4, 13 slices), *yes*$^-$ (n = 4, 14 slices), *src*$^-$ (n = 3, 13 slices), and *abl*$^-$ (n = 2, 9 slices) mice. Paired-pulse facilitation was examined with a 50-ms pulse interval. (**A**) Examples of field EPSP's from wild-type (*wt*) and *fyn*$^-$ mice. (**B**) Histogram shows the ratio of the slope of the second field EPSP to the first field EPSP (mean ± SEM). Calibration bars are 1.5 mV, 22 ms.

S. G. N. Grant, T. J. O'Dell, K. A. Karl, and E. R. Kandel are in the Center for Neurobiology and Behavior, Howard Hughes Medical Institute, College of Physicians and Surgeons of Columbia University, New York, NY 10032. P. L. Stein and P. Soriano are in the Institute for Molecular Genetics, Baylor College of Medicine, and P. Soriano is in the Howard Hughes Medical Institute, Baylor College of Medicine, Houston, TX 77030.

fyn, *yes*, and *abl* genes, which encode four nonreceptor tyrosine kinases, all of which are expressed in the hippocampus (Fig. 1) (*14*). The mutations were engineered by homologous recombination in mouse embryonic stem cells and resulted in no detectable Src, Fyn, or Yes protein and in a truncation in the COOH-terminal region of Abl.

Src, Fyn, Yes, and Abl in the hippocampus. None of the four mouse mutants that we studied has been described as showing an obvious neurological phenotype. Disruption of the *src* gene results in osteopetrosis (*15*). Mutations in *fyn* result in a defect of signal transduction in T cells (*16, 17*). Mice with disruptions in the *abl* gene are runted and depleted in mature T cells and B cells (*18*). Mice lacking *yes* expression have no demonstrable phenotype (*19*).

To examine possible neuronal phenotypes in these mutant mice and to obtain a baseline for subsequent studies of long-term synaptic plasticity and spatial learning, we studied the synaptic connections between the CA3 and the CA1 pyramidal cells. Synaptic transmission in hippocampal slices from each of the mutant mice (*20*) was indistinguishable from that in similar preparations from wild-type mice (*21*). For example, the maximum field excitatory postsynaptic potentials (EPSP's) evoked in slices from *fyn*$^-$ mice were identical to those from wild-type mice. Furthermore, paired-pulse facilitation, a short-term form of synaptic plasticity that results in facilitated transmitter release from the presynaptic terminals, was normal in slices from mutant mice (Fig. 2).

Mice with mutations in the *src*, *yes*, and *abl* genes also had normal LTP (Fig. 3). By contrast, in *fyn* mutants LTP was impaired (Fig. 4A). To ensure that this phenotype was specific to the *fyn* gene and did not result from an additional, random mutation, we examined homozygous mice derived from two independent ES cell clones containing a null *fyn* mutation [*fyn*1 and *fyn*2 (*16*)] created by replacing the second exon of the *fyn* gene with a *neo* gene. The replaced second exon included the initiator ATG and the myristylation sequence necessary for attaching the *fyn* protein to the plasma membrane. We also analyzed the *fyn* mutation on the 129Sv inbred genetic background and on hybrids between 129Sv and C57BL/6J. No differences were detected in the deficiency of LTP between *fyn*1 and *fyn*2 mutants or between inbred mice or those with a hybrid background.

Reduction in LTP in *fyn* mutant mice. LTP was impaired in the CA1 neurons of hippocampal slices from *fyn*$^-$ mice in both the field EPSP (Fig. 4A) and in the population spike (*22*). However, this impairment was not absolute. Although there was, on average, no LTP in the field EPSP (responses 1 hour after tetanic stimulation were 90.5 ± 4.5 percent of control in slices from *fyn*$^-$, $n = 5$, compared to 177.5 ± 2.9 percent of control in slices from wild-type mice, $n = 5$), there was a markedly reduced but nevertheless long-lasting potentiation in some experiments.

In our initial experiments, we adjusted the intensity of presynaptic fiber stimulation in each slice so that field EPSP amplitude elicited would be 1.0 mV (Fig. 4A). To determine whether the apparent lack of LTP in slices from *fyn*$^-$ mice might reflect a change in the threshold for the induction of LTP, we used two different stimulation strengths during the high frequency tetanus. The weak intensity tetanus evoked a postsynaptic response equivalent to 25 percent of the maximal field EPSP. The strong intensity tetanus evoked responses equivalent to 75 percent of the maximal field EPSP. Whereas weak stimulation strengths during a tetanus produced robust LTP in slices from wild-type mice (149.6 ± 18.2 percent), this protocol induced little or no LTP in slices from *fyn*$^-$ mice (108 ± 7.6 percent) (Fig. 4B). However, when strong intensity stimulation was used during the tetanus, a reduced form of LTP (approximately 50 percent of that observed in slices from wild-type animals) was evident (133 ± 9.3 percent in *fyn*$^-$; 168.5 ± 11.6 percent in wild-type) (Fig. 4C). This reduced form of LTP in *fyn*$^-$ slices had the properties of normal LTP. It was blocked by the NMDA receptor antagonist APV (*23*) (Fig. 5C), and it was unaffected by the Ca^{2+} channel blocker nifedipine (*24*).

An even more effective way of activating the NMDA receptor and the subsequent steps in the induction of LTP is to depolarize the postsynaptic cell directly rather than synaptically. We therefore ini-

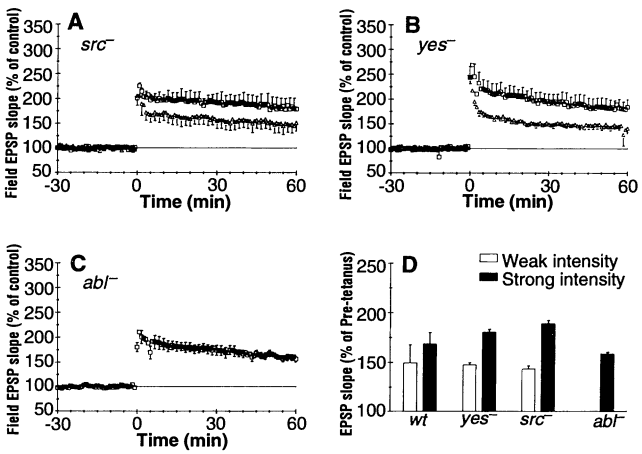

Fig. 3. LTP in hippocampal slices from *src*$^-$ (**A**), *yes*$^-$ (**B**), and *abl*$^-$ (**C**) mice. Squares are results from experiments in which a strong tetanus was used to induce LTP; triangles represent average responses in which LTP was induced with a weak tetanus. (**D**) LTP measured 1 hour after tetanic stimulation. In (A), $n = 3$ animals, 7 slices for the weak tetanus and $n = 2$ animals, 6 slices for the strong tetanus; in (B), $n = 3$ animals, 6 slices for the weak tetanus and $n = 3$ animals, 6 slices for the strong tetanus. Only the strong intensity tetanus was tested in slices from *abl*$^-$ mice [(C), $n = 2$ animals, 7 slices].

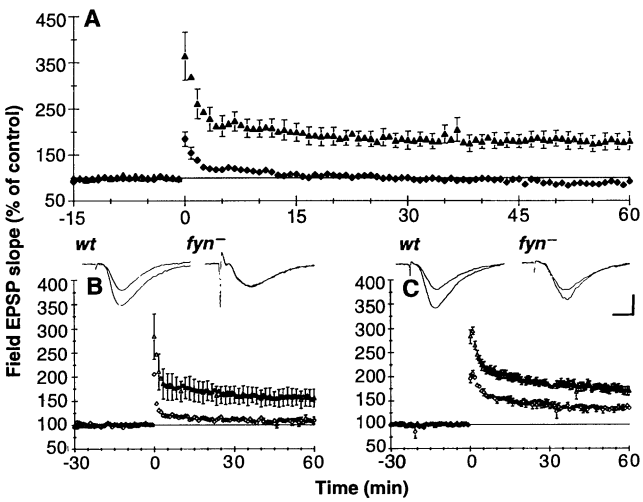

Fig. 4. Impaired LTP in hippocampal slices from *fyn*$^-$ mice. (**A**) Field EPSP slopes recorded before and after tetanic stimulation in slices from *fyn*$^-$ mice (diamonds) or wild-type mice (triangles). Each point shown is the mean ± SEM; $n = 5$ animals, 11 slices for *fyn*$^-$ mice; $n = 5$ animals, 7 slices for wild-type mice. (**B**) Effect of weak (25 percent of maximum) tetanic stimulation in slices from wild-type animals (triangles, $n = 5$, 9 slices) or *fyn*$^-$ mice (diamonds, $n = 3$, 8 slices). Traces are responses elicited just before and 1 hour after tetanic stimulation. Calibration bars are 1 mV, 5.5 ms. (**C**) Effect of strong (75 percent of maximal) tetanic stimulation on LTP in slices from *fyn*$^-$ mice (diamonds, $n = 3$, 8 slices) or control animals (triangles, $n = 4$, 12 slices).

tiated LTP by pairing postsynaptic depolarization with low-frequency presynaptic stimulation. When LTP was induced in this manner, there was no difference in the amount of LTP observed in slices from *fyn*$^-$ and wild-type mice (Fig. 5A).

These experiments indicate that the blunting of LTP in *fyn*$^-$ mice can be overcome by strong inducing stimuli and that, therefore, under these conditions, Fyn is not essential for LTP. Thus, Fyn may have a modulatory role, influencing the threshold for induction of LTP. In fact, LTP induced by pairing the synaptic input with strong postsynaptic depolarization is fully blocked by the tyrosine kinase inhibitor genistein (*25*), suggesting that other tyrosine kinases may contribute to LTP.

The lack of Fyn may lead to a blunting of LTP at weak and moderate intensities of presynaptic stimulation in one of three ways: (i) by altering the functioning of the NMDA receptor; (ii) by impairing the synaptic depolarization that leads to the activation of the NMDA receptor; or (iii) by leading to a less effective recruitment of the steps subsequent to the activation of the NMDA receptor. To assess the contribution of the NMDA receptor to the excitatory postsynaptic current (EPSC), we used whole-cell patch-clamp techniques, optimal conditions for revealing the NMDA receptor component (*20*), and submaximal stimulus intensities. The NMDA receptor component of the excitatory synaptic current in the *fyn*$^-$ mice appeared normal and was indistinguishable from that in wild-type cells (Fig. 5B).

We next examined the possibility that the input pathway did not produce a depolarization sufficient to activate the NMDA receptor optimally. We estimated the magnitude of the synaptic depolarization produced by the tetanic stimulation used to initiate LTP. We measured the area under the field EPSP produced by the tetanus and found no significant difference ($t_{(5)} = 0.94$, not significant) between the depolarization produced by tetanic stimulation (100 Hz, 1-s duration) in slices from *fyn*$^-$ and that from wild-type mice (1886 ± 663.5 mV × ms, $n = 4$ slices from 4 wild-type mice; 1457 ± 480.2 mV × ms, $n = 9$ slices from 3 *fyn*$^-$ mice). We also tested the effectiveness of the input pathway in an independent way by examining its capability to produce PTP. This enhancement of transmitter release normally follows the tetanus to the presynaptic fibers and is of even greater amplitude than that caused by LTP. To produce PTP, we stimulated the Schaffer collateral and commissural fibers with the same high-frequency train of synaptic stimulation used to induce LTP but prevented LTP with the NMDA receptor antagonist APV (50 μM). Under these conditions PTP was normal in *fyn*$^-$ mice (Fig. 5C).

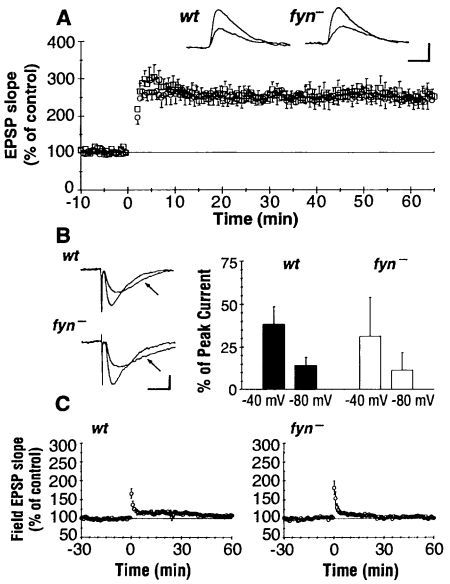

Fig. 5. LTP and NMDA receptor function and PTP in hippocampal slices from *fyn*$^-$ mice. Induction of LTP in hippocampal slices from *fyn*$^-$ mice by pairing 40 EPSP's (evoked at 1 Hz) with depolarization of the postsynaptic cell. (**A**) Results from wild-type mouse CA1 pyramidal cells (squares, mean ± SEM; $n = 10, 11$ cells) and *fyn*$^-$ mouse cells (circles, $n = 7, 11$ cells). One hour after inducing LTP by pairing EPSP's with postsynaptic depolarization, EPSP's were 245.6 ± 22.6 percent of control (mean ± SEM) in cells from wild-type mice whereas EPSP's were 237.6 ± 17.8 percent of control in cells from *fyn*$^-$ mice. Traces show intracellular EPSP's elicited just before and 60 min after inducing LTP in individual experiments from wild-type and *fyn*$^-$ mice. Calibration bars are 5 mV, 15 ms. (**B**) The NMDA component of the excitatory postsynaptic current (EPSC) in *fyn*$^-$ mice. The EPSC's were recorded at two different membrane potentials (−40 and −80 mV), and current amplitude measured 25 ms after the peak current was used to estimate the NMDA component of the EPSC (*4*). The magnitude of the NMDA component of the EPSC, expressed as a percentage of the peak EPSC amplitude, was reduced with membrane hyperpolarization and was of comparable magnitude in cells from both wild-type and *fyn*$^-$ mice. The traces on the left show EPSC's at −80 and −40 mV (arrows) in cells from wild-type and *fyn*$^-$ mice. Calibration bars are 50 pA and 17 ms. (**C**) PTP in slices from *fyn*$^-$ mice. Two trains of strong intensity 100-Hz stimulation (1 s in duration, separated by 20 s) were delivered at time = 0. PTP, measured at the increase in the first response after the last high-frequency train, was 166.5 ± 26.2 percent (mean ± SEM) of control in slices from wild-type mice ($n = 4$ animals, 4 slices) and 181.8 ± 31.3 percent of control in slices from *fyn*$^-$ mice ($n = 3$ animals, 4 slices).

These experiments suggest that the NMDA receptor in *fyn*$^-$ mice functions normally and that the synaptic depolarization of the postsynaptic cells produced by the input seems adequate to activate the NMDA receptor. We find the results most consistent with a modulatory defect in the sequence of steps subsequent to the activation of the NMDA receptor. However, we cannot rule out a developmental abnormality in the spatial arrangement of the synaptic input onto the dendrites of the CA1 cells, which might result in a failure to adequately depolarize the dendritic spines and therefore produce suboptimal activation of the NMDA receptors specifically located in the spines of the apical dendrites (*26*).

Impairment of spatial learning in *fyn*$^-$ mice. To obtain a behavioral measure of the defect in *fyn*$^-$ mice, we examined spatial learning, a form of learning that, in rodents, is dependent on an intact hippocampus (*3*). Blockade of LTP in the hippocampus, with NMDA receptor antagonists, interferes with spatial learning (*27*). Because these blockers may perturb other aspects of synaptic transmission dependent on NMDA receptor functioning unrelated to LTP, we have reexamined this link between spatial learning and LTP genetically, by determining whether the blunting of hippocampal LTP is reflected in an impairment in spatial learning. We first assessed spatial learning in the Morris water maze (*27*), a procedure in which mice placed in a circular pool filled with opaque water escape by swimming and landing on a hidden platform. To learn the location of the hidden platform, the mice must rely on spatial cues provided by several distal visual landmarks surrounding the pool. During a 7-day training period, wild-type mice showed a gradual reduction in the time taken to find the hidden platform ($F_{(6,54)} = 6.31$, $P < 0.01$) (*28*). This reduction did not occur with *fyn*$^-$ mice ($F_{(6,48)} = 0.16$, not significant); their behavior was significantly different from that of wild-type mice ($F_{(6,102)} = 3.45$, $P < 0.01$) (Fig. 6B).

To separate learning from other behavioral changes that contribute to more rapid escape to the hidden platform, we used two transfer tests in which the platform was removed from the pool and the trained mice were allowed to swim freely for 60 s. Mice that have learned the spatial localization of the platform normally spend more time in the quadrant that earlier had contained the missing platform and swim more frequently over the site of the missing platform. In the first transfer test (performed immediately after 7 days of training), the wild-type mice searched primarily in the trained quadrant (Fig. 6, C and D). By contrast, the *fyn*$^-$ mice spent no more time

in the quadrant that had contained the platform than would be expected by chance (13.1 ± 3.4 s, not significant). When the transfer test was repeated 5 days later (day 12), the wild-type mice showed a slight improvement in performance, perhaps as a result of the reinstatement training after the previous transfer test, and performed significantly better than would be expected by chance (24.1 ± 3.6 s, $P < 0.05$) (Fig. 6D). The *fyn*$^-$ mice again failed to show learning (14.3 ± 3.6 s, not significant). The wild-type mice crossed the area where the platform had been more frequently than did the *fyn*$^-$ mice, suggesting that the *fyn*$^-$ mice failed to learn the spatial location of the escape platform (crossings per trial: wild type = 2.4 ± 0.8, *fyn*$^-$ = 1.4 ± 0.9).

The apparent loss of spatial learning in the *fyn*$^-$ mice might result from impaired vision or swimming ability or lack of motivation. To examine these parameters, we conducted a control experiment in which the mice learned, during an 8-day training period, to swim to the platform now made visible by placing a flag on top. In this case, distal visual cues are absent so that the learning task does not require a spatial map; rather, the mice need only to learn an association with a single cue. In this visual learning task, both *fyn*$^-$ ($F_{(7,56)} = 10.62$, $P < 0.01$) and wild-type mice ($F_{(7,63)} = 2.36$, $P < 0.05$) improved during the 8 days of training. Although the wild-type mice initially performed with a lower escape latency (wild type: 17.6 ± 4.2 s; *fyn*$^-$: 37.1 ± 4.7 s, $P < 0.01$), the *fyn*$^-$ mice improved sufficiently by day 6 so that they performed as well as wild-type mice (wild type: 11.4 ± 3.5 s; *fyn*$^-$: 16.1 ± 4.6 s, not significant). This result demonstrates that *fyn*$^-$ mice can learn some tasks and suggests that the deficit in spatial learning in *fyn*$^-$ mice is specific and unlikely to result from an inability to perform in the water maze (*29*).

Role of Fyn in the development of the hippocampal neural circuitry. The finding that there is normal synaptic transmission, paired-pulse facilitation, and PTP but a blunted form of LTP in the *fyn*$^-$ mice is consistent with the idea that the Fyn may modulate the induction of LTP and contribute to spatial learning. However, the link between Fyn, LTP, and learning may arise through an alternative mechanism. The *fyn* mutation could result in a developmental abnormality in the circuitry of the hippocampus leading to a blunting of LTP and of learning in the adult animal. To explore this possibility, we surveyed the brain histologically, focusing in particular on the neocortex, hippocampus, and cerebellum. In these three regions, we found no gross abnormality in the overall arrangements of cells or fiber tracts. In the cerebral cortex, for example, there is a cellular representation for each whisker in the form of barrel fields (*30*). These barrel fields were normal in appearance in *fyn*$^-$ mice (Fig. 7A).

Although the gross architecture of the hippocampus in *fyn*$^-$ mice was normal, we found a clear defect in the arrangement of the granule cells of the dentate gyrus and in that of their target cells, the pyramidal cells of the CA3 region (Fig. 7B). These defects were specific to *fyn*$^-$ mice and were not present in *src*$^-$, *yes*$^-$, or *abl*$^-$ mice but were present in both *fyn*1 and *fyn*2 mice and in both inbred and hybrid strains. This abnormality is evident as an undulation in the granule cell layer in the dentate gyrus and in the pyramidal cell layer in region CA3 (Fig. 7B). In the CA3 region, the undulation of the cell layer was more prominent in caudal (ventral) than in rostral (dorsal) regions of the hippocampus. Counting of pyramidal cells in the caudal CA3 region and dendate gyrus granule cells in the rostral region of *fyn*$^-$ mice indicates that these undulations reflect an increase of 25 percent in cell number compared to wild-type mice (CA3: *fyn*$^-$, 260 ± 14; wild type, 206 ± 8; $P < 0.02$. Dendate gyrus: *fyn*$^-$, 379 ± 21; wild type, 275 ± 16; $P < 0.01$; mean ± SEM) (*31*). This increase in neuron number may result from overproliferation, altered cell fates, or failure of cell death.

To examine the mossy fiber pathway that connects the granule cells to the CA3 region, we used the Timm stain, which selectively stains this pathway. Despite the fact that both the granule cell layer and the layer of CA3 pyramidal cells display undulations, the mossy fiber pathway appears normal in its overall projections (Fig. 7C). In the CA1 region of the hippocampus, there is a characteristic cholinergic fiber pathway. The pattern of this innervation also was normal in *fyn*$^-$ mice (Fig. 7D).

The primary targets of the CA3 neurons are the apical dendrites of CA1 pyramidal neurons (*32*), and the LTP we have studied is produced at the synapses that the CA3 cells make with the CA1 neurons. We therefore examined the morphological integrity of the apical dendrites of the CA1 pyramidal neurons. Immunohistochemical detection of a dendritic-specific protein, the microtubule-associated protein 1 (MAP1), revealed that the apical dendrites are present and extend across the full width of the stratum radiatum but appear less tightly organized than in wild type (Fig. 7E). It is not clear whether this change is primary or secondary to a change in the packing density of the CA1 pyramidal cells,

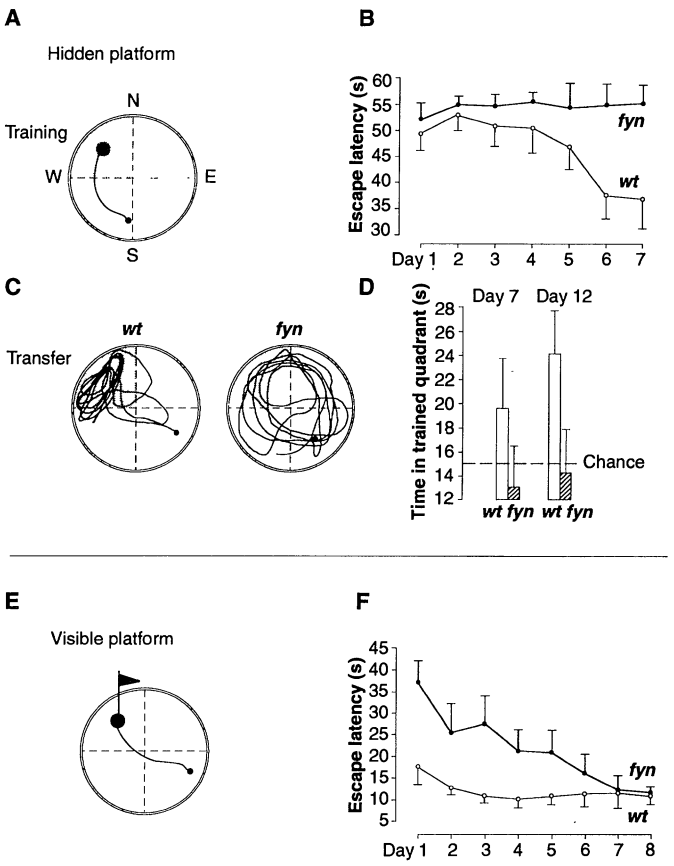

Fig. 6. Impaired learning of *fyn*$^-$ mice in the water maze. (**A**) Escape latency to a hidden platform (*45*). Mice were trained for seven consecutive days to swim from random locations to a hidden platform in a fixed location (stippled circle in shaded northwest quadrant). The time required for the mouse to escape (escape latency) was recorded on each day (**B**). Transfer test (**C** and **D**). After 7 days of training, the platform was removed and the mice were allowed to swim for 60 s. Individual examples (C) show records of a wild-type mouse searching in the quadrant that had contained the platform (shaded) and a *fyn*$^-$ mouse swimming randomly (D). Visible platform training (**E** and **F**) (*46*). Path of a mouse trained to reach the randomly located flagged platform (E). The escape latency was recorded for eight consecutive days of training (F). Mean and SEM are shown for nine *fyn*$^-$ mice and ten wild-type mice all on a 129Sv strain background.

which do not appear to form as tight a layer in the *fyn* mutants as in the wild type.

Because the pyramidal cells of the CA3 region that give rise to the presynaptic afferents to CA1 show a disorganized arrangement, a developmental abnormality in the spatial organization of synaptic inputs onto the apical dendrites of the CA1 cells could contribute to the blunting of LTP and spatial learning. Nevertheless, this afferent pathway seems intact physiologically. It is capable of normal synaptic transmission, short-term synaptic plasticity, and, under some conditions, LTP. Thus, the defect in LTP may arise from an independent abnormality in the mature functioning synapse, but we cannot fully distinguish between these two possibilities.

A role for *fyn* in development and plasticity. If Fyn is important for LTP, it should be present in the mature synapse (*8*). In subcellular fractionation studies (Fig. 8), we found that Fyn was present in synaptosomes and was enriched in the synaptic plasma membranes and in the postsynaptic density, where Ca^{2+}/calmodulin-dependent protein kinase II (CamKII) also is enriched. A similar pattern of expression was found for Src (*33*) and Yes. Thus, our data are consistent with the idea that although Fyn is important in the development of the hippocampus it may also have a role in the mature synapse related to

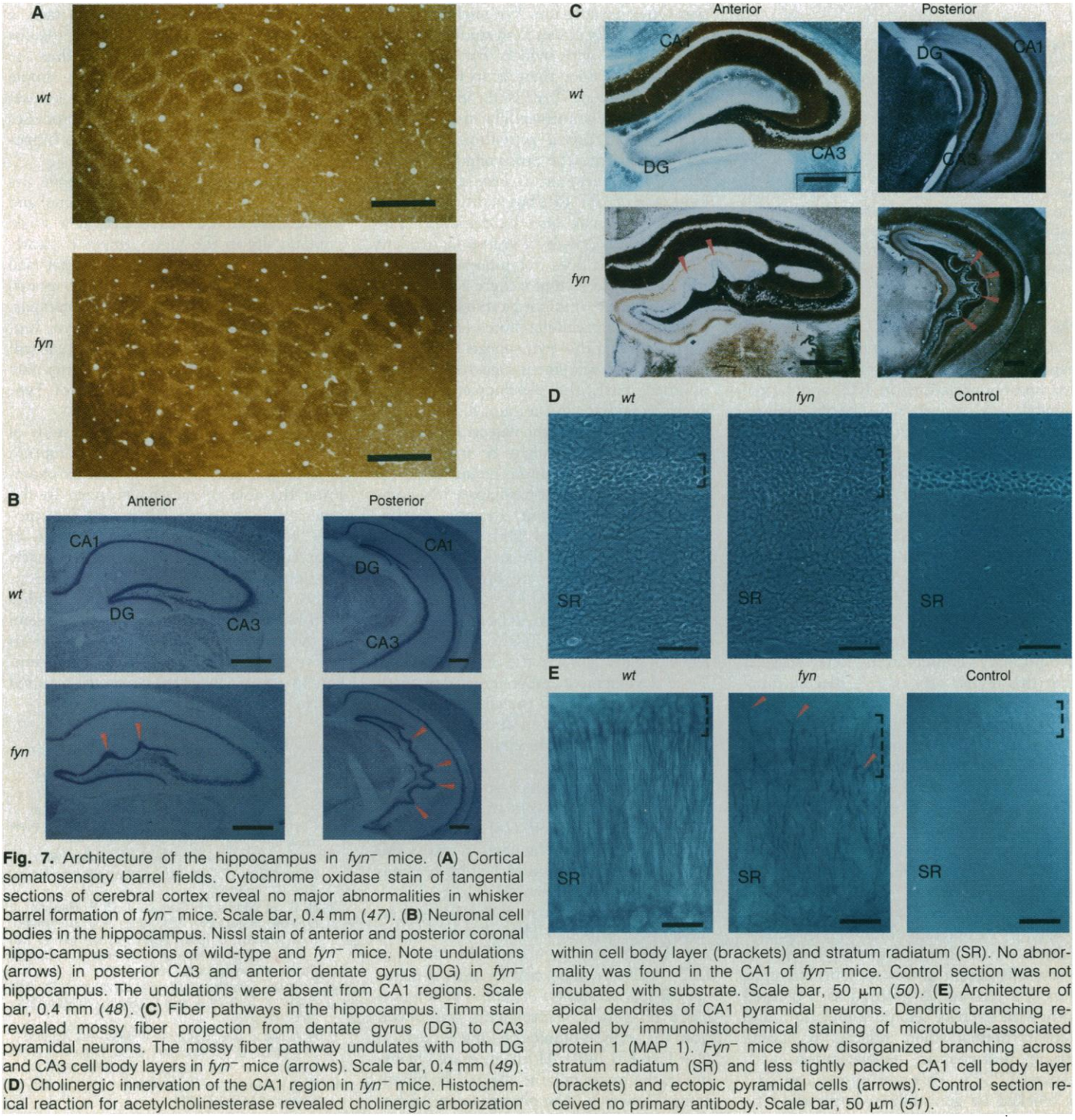

Fig. 7. Architecture of the hippocampus in *fyn*⁻ mice. (**A**) Cortical somatosensory barrel fields. Cytochrome oxidase stain of tangential sections of cerebral cortex reveal no major abnormalities in whisker barrel formation of *fyn*⁻ mice. Scale bar, 0.4 mm (*47*). (**B**) Neuronal cell bodies in the hippocampus. Nissl stain of anterior and posterior coronal hippo-campus sections of wild-type and *fyn*⁻ mice. Note undulations (arrows) in posterior CA3 and anterior dentate gyrus (DG) in *fyn*⁻ hippocampus. The undulations were absent from CA1 regions. Scale bar, 0.4 mm (*48*). (**C**) Fiber pathways in the hippocampus. Timm stain revealed mossy fiber projection from dentate gyrus (DG) to CA3 pyramidal neurons. The mossy fiber pathway undulates with both DG and CA3 cell body layers in *fyn*⁻ mice (arrows). Scale bar, 0.4 mm (*49*). (**D**) Cholinergic innervation of the CA1 region in *fyn*⁻ mice. Histochemical reaction for acetylcholinesterase revealed cholinergic arborization within cell body layer (brackets) and stratum radiatum (SR). No abnormality was found in the CA1 of *fyn*⁻ mice. Control section was not incubated with substrate. Scale bar, 50 μm (*50*). (**E**) Architecture of apical dendrites of CA1 pyramidal neurons. Dendritic branching revealed by immunohistochemical staining of microtubule-associated protein 1 (MAP 1). *Fyn*⁻ mice show disorganized branching across stratum radiatum (SR) and less tightly packed CA1 cell body layer (brackets) and ectopic pyramidal cells (arrows). Control section received no primary antibody. Scale bar, 50 μm (*51*).

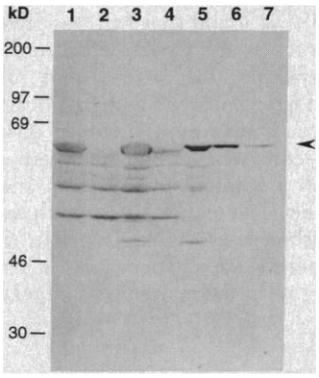

Fig. 8. Synaptic expression of Fyn (arrow). Protein immunoblot with antibody to Fyn of proteins from wild-type whole brain (lane 1), whole brain from *fyn*$^-$ mice (lane 2), or synaptosomes from wild-type mice (lane 3). Synaptosomes from wild-type mice were fractionated into soluble (lane 4) and insoluble (synaptic junctional complex, lane 5) fractions. The synaptic junctional complex was fractionated further into postsynaptic densities (lane 6) and synaptic plasma membranes (lane 7). Equal proportions of the fractions from synaptosomes were loaded (*52*).

the induction of LTP.

Of the mice lacking one of four nonreceptor tyrosine kinases, only those lacking *fyn* had abnormalities in LTP and hippocampal development. The specific requirement for Fyn may result from structural and regulatory features that distinguish it from other members of the Src family. Kinases of the Src family have three major domains defined by function and sequence similarity—a distinguishing NH_2-terminal domain is followed by the highly conserved noncatalytic Src homology domains (SH2 and SH3) and by the COOH-terminal catalytic domain (SH1) (*11*). Although this NH_2-terminal domain differs among members, its evolutionary conservation here suggests that this region may have a specific function (*34*), such as the association with a membrane receptor or regulation of kinase function (*35*). Many members of the Src family are often associated with or activated by a single receptor (*36*), suggesting that several Src family kinases may participate in a common signaling pathway. In LTP, the distinct regulatory properties of the individual kinases might give rise to distinctive activation thresholds.

As would be expected, in view of the possibility of different thresholds of activation, we found that LTP in the *fyn*$^-$ mice is essentially absent at low stimulus strengths during a tetanus, is induced as a blunted form with stronger tetanic stimulation, and appears normal when induced by pairing strong postsynaptic depolarization with evoked EPSP's. This pairing-induced LTP is blocked by genistein in both wild-type and *fyn*$^-$ mice, indicating that tyrosine kinases other than *fyn* participate in LTP (*25*). This raises the possibility that under conditions of higher intensity stimulation, other related tyrosine kinases may overcome the Fyn deficiency. This idea could be tested with double mutant mice containing deficiencies in Fyn and Yes or Src.

Tyrosine kinases in the postsynaptic cell appear to contribute to the induction rather than the maintenance phase of LTP (*8*). This idea is consistent with the evidence that Fyn is enriched in postsynaptic densities. One clue as to how Fyn might function postsynaptically comes from studies of the T cell receptor with which Fyn associates (*13*). In *fyn*$^-$ mice there is an impairment in the ability of T cells to increase the concentration of intracellular free Ca^{2+} in response to receptor activation (*16*, *17*). Ca^{2+} influx into the postsynaptic cell, via the NMDA receptor, is necessary for the induction of LTP (*6*), but additional sources of Ca^{2+} may also be required. The finding that blockade of voltage-dependent Ca^{2+} channels does not influence LTP in *fyn*$^-$ mice suggests that if there is a defect in Ca^{2+} handling, it might be in the release of Ca^{2+} from intracellular stores (*38*).

The finding that Fyn appears to function in neuronal development suggests three possibilities. First, the developmental defect might be primary and account for the blunting of LTP. Second, the defects in development and in LTP might be independent reflections of a common requirement for Fyn. Third, Fyn might participate in a common activity-dependent synaptic mechanism that is required both for neuronal development and for the synaptic plasticity of learning. Because the final number of pyramidal cells in the CA3 region but not in the CA1 region appears to be determined by cell death (*39*), Fyn might participate in regulating cell death in the hippocampus. In T cell development, programmed cell death requires an increase in the concentration of free intracellular Ca^{2+} that occurs after activation of the T cell receptor (*37*). In *fyn*$^-$ thymocytes in which Ca^{2+} fluxes are attenuated, the ability to undergo cell death in response to certain types of antigens also appears to be impaired (*16*). Perhaps Fyn may determine cell number in the CA3 region and dentate gyrus of the hippocampus by an analogous mechanism.

Mutations in the *fyn* gene result in an impairment of both LTP and spatial learning. This is consistent with the idea that LTP is causally important for storing memory for spatial events. A similar conclusion based on genetic experiments was drawn from the analysis of mice lacking expression of α-CamKII (*40*). Although spatial learning in the water maze is affected by hippocampal lesions and by pharmacological manipulations that block LTP, it is important to emphasize that our experiments do not exclude the possibility that the impaired learning may result from a lack of gene expression outside the hippocampus. Indeed, both Fyn and CamKII (*41*) are expressed in the neocortex, the cerebellum, and other regions of the brain. Moreover, spatial learning can be disrupted by lesions outside the hippocampus, in particular by lesions of the entorhinal area and of the frontal cortex (*42*). In fact, both the *fyn*$^-$ and CamKII$^-$ mice show an initial impairment in the single-cue association task, a task that requires nonhippocampal regions (*43*). This finding suggests either that the hippocampus can be involved in simple associative learning or that these kinases may be important for learning processes that require regions other than the hippocampus.

The correlation we describe above between the learning deficit in the animal and a deficiency in LTP examined at a single synaptic site in the hippocampus is clearly only a first step in an analysis that will require examination of other relay points both within and outside the hippocampus. To strengthen the links between Fyn, hippocampal LTP, and spatial learning, it will also be necessary to specifically manipulate the expression of mutant forms of Fyn, restricted only to the hippocampus.

In addition to their role in the study of behavior and learning, targeted disruption of genes provides a powerful tool for examining the role of specific proteins in the function of the brain. Thus, our data provide initial insights into the function of nonreceptor tyrosine kinases in synaptic plasticity and in hippocampal development. A combination of genetic studies with biochemical analyses should be useful for the delineation of the specific functions of Fyn and perhaps other Src family members in the biochemical pathways required for the induction of LTP.

REFERENCES AND NOTES

1. Y. Dudai, *Annu. Rev. Neurosci.* 11, 537 (1988); R. L. Davis and B. Dauwilder, *Trends Genet.* 7 (no. 7), 224 (1991); M. Heisenberg, in *Progress in Zoology*, G. Rahmann, Ed. (Fisher-Verlag, New York, 1989), pp. 3–45.
2. L. R. Squire, *Psychol. Rev.* **99**, 195 (1992); H. Eichenbaum, T. Otto, N. J. Cohen, *Behav. Neural Biol.* **57**, 2 (1992).
3. R. G. M. Morris, P. Garrud, J. N. P. Rawlins, J. O'Keefe, *Nature* **297**, 681 (1982); R. J. Sutherland, I. Q. Wishaw, B. Kolb, *Behav. Brain Res.* 7, 133 (1983); H. Eichenbaum, P. Mathews, N. J. Cohen, *Behav. Neurosci.* **103**, 1207 (1989).
4. T. Lømo, *Acta Physiol. Scand.* **68** (supp. 277), 128 (1966); T. V. P. Bliss and T. Lømo, *J. Physiol.* **232**, 331 (1973).
5. R. A. Nicoll, J. A. Kauer, R. C. Malenka, *Neuron* 1, 97 (1988); D. V. Madison, R. C. Malenka, R. A. Nicoll, *Annu. Rev. Neurosci.* **14**, 379 (1991).
6. G. L. Collingridge, S. J. Kehl, H. McLennan, *J. Physiol.* **334**, 33 (1983).

7. R. Malinow, D. V. Madison, R. W. Tsien, *Nature* **335**, 820 (1988); R. Malinow, H. Schulman, R. W. Tsien, *Science* **245**, 862 (1989); R. C. Malenka *et al.*, *Nature* **349**, 554 (1989).
8. T. J. O'Dell, E. R. Kandel, S. G. N. Grant, *Nature* **353**, 558 (1991).
9. H. Bading and M. E. Greenberg, *Science* **253**, 912 (1991).
10. T. J. O'Dell, R. D. Hawkins, E. R. Kandel, O. Arancio, *Proc. Natl. Acad. Sci. U.S.A.* **88**, 11285 (1991); E. M. Schuman and D. V. Madison, *Science* **254**, 1503 (1991); J. H. Williams, M. L. Errington, M. A. Lynch, T. V. P. Bliss, *Nature* **341**, 739 (1989); J. E. Haley, G. L. Wilcox, P. F. Chapman, *Neuron* **8**, 211 (1992); G. A. Bohme *et al.*, *Eur. J. Pharmacol.* **199**, 379 (1991).
11. J. A. Cooper, in *Peptides and Protein Phosphorylation*, B. Kemp and P. F. Alewood, Eds. (CRC Press, Boca Raton, FL, 1989), pp. 85–113; C. A. Koch, D. Anderson, M. F. Moran, C. Ellis, T. Pawson, *Science* **252**, 668 (1991).
12. R. Ralston and J. M. Bishop, *Proc. Natl. Acad. Sci. U.S.A.* **82**, 7845 (1985); K. Gould and T. Hunter, *Mol. Cell Biol.* **8**, 3345 (1988); R. M. Kypta, Y. Goldberg, E. T. Ulug, S. A. Courtneidge, *Cell* **62**, 481 (1990).
13. L. E. Samelson, A. F. Phillips, E. T. Luong, R. D. Klausner, *Proc. Natl. Acad. Sci. U.S.A.* **87**, 4358 (1990); A. Y. Tsygankov, B. M. Broker, J. Fargnoli, J. A. Ledbetter, J. B. Bolen, *J. Biol. Chem.* **267**, 18259 (1992).
14. M. M. Sugrue *et al.*, *J. Neurosci.* **10**, 2513 (1990); Y.-H. Zhao, H. Baker, S. I. Walaas, M. Sudol, *Oncogene* **6**, 1725 (1991).
15. P. Soriano, C. Montgomery, R. Geske, A. Bradley, *Cell* **64**, 693 (1991).
16. P. L. Stein, H.-M. Lee, S. Rich, P. Soriano, *ibid.* **70**, 741 (1992).
17. M. K. Appleby *et al.*, *ibid.*, p. 751.
18. P. L. Schwartzberg *et al.*, *ibid.* **65**, 1165 (1991); V. L. J. Tybulewicz, C. E. Crawford, P. K. Jackson, R. T. Bronson, R. C. Mulligan, *ibid.*, p. 1153.
19. P. Soriano, unpublished data.
20. Mouse brains were removed from the skull and placed in an ice-cold (0° to 4°C) artificial cerebrospinal fluid (ACSF) containing 124 mM NaCl, 4.4 mM KCl, 25 mM $NaHCO_3$, 1.0 mM $Na_2H_2PO_4$, 2.0 mM $CaCl_2$, 2.0 mM $MgSO_4$, or $MgCl_2$, and 10 mM glucose, with 50 to 80 μM, D,L-2-amino-5-phosphonovaleric acid (APV). Hippocampal slices (400 μm thick) were transferred to an interface recording chamber containing cool ACSF with APV (15° to 20°C). APV-free ACSF was perfused through the chamber (1 to 3 ml/min) as the temperature in the recording chamber was slowly increased to 30°C. Electrophysiological experiments were begun after waiting at least 1.5 hours for the slices to recover. A fine, platinum and iridium bipolar stimulating electrode was used to stimulate Schaffer collateral and commissural fibers in the stratum radiatum of the CA1 region of the hippocampus. In field potential recordings, synaptic responses were elicited at 0.02 Hz and responses were recorded with low resistance (5 to 10 megohm) glass microelectrodes filled with either 2.5 M NaCl or ACSF. When synaptic potentials were recorded intracellularly, high resistance (40 to 120 megohm) microelectrodes filled with 2 to 3 M CsCl were used, and the presynaptic fibers were stimulated at 0.1 Hz. Tetanus-induced LTP was elicited with trains (1 s) of 100-Hz stimulation delivered twice with an intertrain interval of 20 s. When EPSP's were recorded intracellularly, picrotoxin (50 to 100 μM) was added to the ACSF, the concentrations of $CaCl_2$ and $MgSO_4$ were increased to 4.0 mM, and the CA3 region of the hippocampus was removed. Constant hyperpolarizing currents were used to maintain the membrane potentials between −80 and −90 mV, and the intensity of presynaptic stimulation (0.02-ms duration pulse) was adjusted to elicit EPSP's of between 3 and 7 mV. In experiments in which LTP was induced by injecting current, we depolarized the membrane potential to between −20 and −10 mV. Once the Ca^{2+} spikes elicited by this depolarization had subsided, we paired 40 EPSP's evoked at 1.0 Hz. Excitatory postsynaptic currents were recorded with the "blind" whole-cell voltage-clamp technique described by Blanton *et al.* [*J. Neurosci. Methods* **30**, 203 (1989)]. Patch clamp electrodes (5 to 10 megohm resistance) were filled with a solution containing: 130 mM $CsCH_3SO_3$, 5 mM $MgCl_2$, 0.5 mM EGTA, 0.05 mM $CaCl_2$, 10 mM Hepes, and 2.0 mM adenosine triphosphate (pH = 7.3, adjusted with CsOH). The bath solution had the same composition as the ASCF described above except that 50 to 100 μM picrotoxin was added to inhibit inhibitory synaptic currents and the concentrations of Ca^{2+} and Mg^{2+} were 2.5 and 1.4 mM.
21. For example, the maximal field EPSP amplitudes that could be evoked in slices from *fyn*$^-$ mice (5.7 ± 1.1 mV, n = 8 animals, 25 slices) were not significantly different from those recorded from slices from wild-type animals (5.6 ± 1.0 mV, n = 8 animals, 25 slices).
22. We also examined LTP of the population spike, an extracellular potential generated by the nearly simultaneous firing of action potentials in the postsynaptic CA1 pyramidal cells after presynaptic fiber stimulation. In these experiments, the population spike amplitudes in wild-type mice were 391 ± 83.1 percent of those in untreated slices (mean ± SEM, n = 3 animals, 5 slices), and in *fyn*$^-$ mice the responses were 202.1 ± 68.2 percent of control (n = 3 animals, 5 slices).
23. Field EPSP's, 1 hour after tetanic stimulation in 50 μM APV were 102.2 ± 2.3 percent of control (mean ± SEM, n = 3 animals, 4 slices).
24. Field EPSP's were 128.7 ± 2.3 percent of control (mean ± SEM, n = 4 animals, 7 slices) 1 hour after tetanic stimulation in the presence of 20 μM nifedipine compared to 133.2 ± 9.3 percent of control in untreated slices from *fyn*$^-$ mice. In wild-type animals, responses were 161.4 ± 1.5 percent of control (n = 5 animals, 10 slices) 1 hour after tetanus in the presence of nifedipine compared to 168.5 ± 11.6 percent in untreated slices.
25. T. J. O'Dell, unpublished data.
26. T. H. Brown, A. M. Zador, Z. F. Mainen, B. J. Claiborne, in *Long-Term Potentiation*, M. Baudry and Joel L. David, Eds. (MIT Press, Cambridge, MA, 1991), pp. 357–391.
27. R. G. M. Morris, *J. Neurosci.* **9**, 3040 (1989); ———, E. Anderson, G. S. Lynch, M. Baudry, *Nature* **319**, 774 (1986).
28. Statistical tests included one-way and two-way analyses of variance and Student's t test.
29. We observed learning deficits with both hybrid and inbred mice. Whereas the morphological and physiological deficits in LTP were unaffected by genetic background, we found, as has been reported by others, that spatial learning in the water maze in mice appeared to vary with genetic backgrounds. To minimize the effects of genetic background, we used inbred mice (the 129v strain) in all of the experiments; H.-P. Lipp *et al.*, *Experientia* **45**, 845 (1989); M. Upchurch and J. M. Wehner, *Behav. Genet.* **18**, 55 (1988); *Behav. Neurosci.* **6**, 1251 (1989). We used a training procedure that avoided overtraining the mice because, in pilot experiments, overtraining masked the *fyn*$^-$ learning defect.
30. T. A. Woolsey and H. Van der Loos, *Brain Res.* **17**, 205 (1970); C. Welker, *ibid.* **26**, 259 (1971).
31. Three Nissl-stained coronal cryosections (15 μm) (*47*) from posterior hippocampal regions were chosen from each of *fyn*$^-$ and wild-type mice, and two equal-length regions of CA3 pyramidal cells were photographed for counting from each section. Because most cresyl violet–stained CA3 cells are neuronal and the morphology of individual cells was not different between wild-type and *fyn*$^-$ mice, we counted all large nucleated cells. Similarly anterior coronal sections were chosen for counting dentate gyrus cells.
32. N. Ishizuka, J. Weber, D. G. Amaral, *J. Comp. Neurol.* **295**, 580 (1990).
33. S. B. Cudmore and J. W. Gurd, *J. Neurochem.* **57**, 1240 (1991).
34. G. Hannig, S. Ottilie, M. Schartl, *Oncogene* **6**, 361 (1991)
35. J. Y. Kato *et al.*, *Mol. Cell. Biol.* **6**, 4195 (1986); P. C. Espino *et al.*, *Oncogene* **5**, 282 (1990); S. H. Cheng *et al.*, *J. Virol.* **65**, 170 (1991).
36. R. M. Kypta, Y. Goldberg, E. T. Ulug, S. A. Courtneidge, *Cell* **62**, 481 (1990); A. L. Burkhardt, M. Brunswick, J. B. Bolen, J. J. Mond, *Proc. Natl. Acad. Sci. U.S.A.* **88**, 7410 (1991); M. A. Campbell and B. M. Sefton, *Mol. Cell. Biol.* **12**, 2315 (1992).
37. E. D. Hsi *et al.*, *J. Biol. Chem.* **264**, 10836 (1989); T. H. Finkel, P. Marrack, J. W. Kapler, R. T. Kubo, J. C. Cambier, *J. Immunol.* **142**, 3006 (1989); C. H. June, M. C. Fletcher, J. A. Ledbetter, L. E. Samuelson, *ibid.* **144**, 1591 (1991).
38. J. Harvey and G. L. Collingridge, *Neurosci. Lett.* **139**, 197 (1992).
39. B. D. Boss, K. Turlejski, B. B. Stanfield, W. M. Cowan, *Brain Res.* **406**, 280 (1987).
40. A. J. Silva, R. Paylor, J. M. Wehner, S. Tonegawa, *Science* **257**, 206 (1992); A. J. Silva, C. F. Stevens, S. Tonegawa, Y. Wang, *ibid.*, p. 201.
41. K. Fukunaga, S. Goto, E. Miyamoto, *J. Neurochem.* **51**, 1070 (1988).
42. R. J. Sutherland, B. Kolb, I. Q. Whishaw, *Neurosci. Lett.* **31**, 271 (1982).
43. Pharmacological lesions of the hippocampus that result in spatial learning deficits can be masked by overtraining, which is thought to recruit additional brain regions [R. G. M. Morris, *Cold Spring Harbor Symp. Quant. Biol.* **50**, 161 (1985)]. Pilot studies with more intensive training regimens suggest that *fyn*$^-$ mice can learn the spatial task, which together with the results from the visual-cue task may indicate that overtraining permits redundant neural mechanisms to compensate for learning deficits.
44. Frozen hippocampi from six wild-type mice were lysed and immunoprecipitated with antibodies to Fyn (provided by J. Bolen, 2 μl), Src (Oncogene Science, 1 μg), Yes (provided by J. Bolen, 5 μl), or Abl (Oncogene Science Ab-3, 1 μg), and immunecomplex kinase assays were done (*33*). The Abl immunoprecipitation shows two nonspecific bands (50 and 60 kD) that are also seen in assays with preimmune serum exposed overnight.
45. To train mice to swim to a hidden platform in the water maze, we used a 1.2-m (diameter) pool filled with milk maintained at 28°C. The platform was 10 cm in diameter and submerged by 0.5 to 1 cm. The pool was surrounded with a circular white wall printed with dark blue patterns (stars, stripes, shapes) that served as spatial cues. The day before training, mice were given a 60-s swim and allowed to mount the hidden platform three times. Nine *fyn*$^-$ mice (six male, three female) and ten wild-type mice (seven male, three female), all 7 to 9 weeks of age, were tested in a single blind analysis and were randomly assigned for training to find the hidden platform in a given quadrant (NW, NE, SE, or SW). For seven consecutive days, each mouse was placed in the pool four times starting at each of north, south, east, or west locations in a random order, with a 1-hour interval between trials. After locating the platform the mice were allowed to sit for 60 s before being returned to their cage. If after 60 s in the pool, the mice had not located the platform, they were placed on it and escape latency was scored as 61. Transfer tests: Mice were placed in the pool starting at the location opposite the site where the platform had been and allowed to swim for 60 s. The time spent swimming in each quadrant and the number of crossings of the platform site were recorded (as indices of spatial learning). After the transfer test on day 7, the mice were given four reinstatement trainings (maximum 60 s of swimming and 30 s on platform, from each of the four swim start sites). All data were videotaped and analyzed blind. No difference was observed between males and females in any task. Mice were housed in individual cages on a 12-hour light-dark cycle (light 7 a.m. to 7 p.m.) and were tested between 10 a.m. and 5 p.m. Animal care was in accordance with institutional guidelines.

46. Visible platform training: The cues were removed and the location of the platform was made visible by a 6-inch-high mast topped with a circular blue cylinder (5 cm tall by 4 cm diameter). This flag was equally visible from all pool locations. The same mice used in the hidden platform training were trained to swim toward the platform at random locations with six consecutive trainings for eight consecutive days. They were allowed to swim for a maximum of 60 s and to remain on the platform for 30 s.
47. The cerebral cortices fixed in paraformaldehyde were pressed flat in 30 percent sucrose–phosphate-buffered saline (PBS) for 24 hours. The parietal region was freeze mounted and cryostat sectioned (15 μM). The slides were incubated in cytochrome oxidase solution (0.5 mg/ml diaminobenzidine, 0.3 mg/ml cytochrome C, 0.2 mg/ml catalase) overnight at room temperature.
48. Paraformaldehyde-fixed brains were cryosectioned (15 μM) and stained with cresyl violet (0.5 percent).
49. Mice were perfused first with 0.36 percent sodium sulfide in phosphate buffer (10 min) and then neutral buffered formalin (15 min) and processed according to R. S. Sloviter [*Brain Res. Bull.* **8**, 771 (1982)].
50. The acetylcholinesterase histochemistry was carried out on 50 μM vibratome sections; M. J. Karnovsky and L. J. Roots, *Histochem. Cytochem.* **12**, 219 (1969).
51. Brains fixed with paraformaldehyde (4 percent) were sectioned with a vibratome (50 μM) and transferred to 24-well culture dishes. After hydrogen peroxide (0.3 percent) incubation (15 minutes), sections were washed and then blocked in 10 percent goat serum, 0.1 percent Triton X-100 in PBS for 1 hour. Sections were incubated with the MAP1 mouse monoclonal antibody (Sigma) (1:100 dilution) overnight at 4°C. After washing, the sections were incubated in horseradish peroxidase–conjugated antibody to mouse immunoglobulin G (Boehringer) diluted 1:200 in ×0.5 block for 1 to 2 hours. Three further washings preceded DAB development with glucose oxidase.
52. A P2 fraction was prepared from six wild-type mouse brains according to J. W. Gurd, P. Gordon-Weeks, and W. H. Evans [*J. Neurochem.* **39**, 1117 (1982)] Synaptosomes were prepared with the Percoll gradient method of P. R. Dunkley, P. E. Jarvic, J. W. Heath, G. J. Kidd, and J. A. P. Rostas [*Brain Res.* **372**, 115 (1986)] and lysed in tris-acetate (5 mM, pH 8.0) and centrifuged at 30,000*g* for 30 minutes. The supernatant was concentrated by ultrafiltration to 2 ml (synaptosome soluble). The sedimented material was resuspended in 1.5 ml of tris-acetate (synaptic junctional complex), and 50 mM Hepes (pH 7.5) with protease inhibitors and Triton X-100 was added to 10 ml and 1 percent, respectively. After motor homogenization, gentle agitation for 20 minutes and rehomogenization, the extract was centrifuged at 100,000*g* for 30 minutes. The supernatant (synaptic plasma membranes) was concentrated to 4 ml by ultrafiltration, and the sedimented material (postsynaptic density) was resuspended in 1 ml of Hepes. Samples containing 0.4 percent of each fraction were subject to immunoblotting with antiserum to pp59^{fyn} according to manufacturers instruction (UBI).
53. We thank R. Axel and T. Jessell for comments on earlier drafts of this manuscript; R. Hawkins, I. Kupfermann, and R. Morris for advice on behavior experiments and their statistical analyses; B. Stanfield, D. Amaral, and J. Dodd for help on the anatomy; M. Osman and D. Burton for animal care; S. Mack and C. Lam for figures; H. Ayers and A. Krawetz for preparation of the manuscript; S. Goff for *abl*$^-$ mice; and J. Bolen for *fyn* and *yes* antisera. Supported by NIMH grant MH45923, NIHA grant AG08702, and NICHD grants HD24875 and HD25326; by NIH postdoctoral fellowship HD07453 (P.L.S.); and by the Howard Hughes Medical Institute (E.R.K.; P.S., T.J.O., and S.G.N.G).

28 September 1992; 25 November 1992

Selection of a Ribozyme That Functions as a Superior Template in a Self-Copying Reaction

Rachel Green and Jack W. Szostak

The *sunY* ribozyme is derived from a self-splicing RNA group I intron. This ribozyme was chosen as a starting point for the design of a self-replicating RNA because of its small size. As a means of facilitating the self-replication process, the size of this ribozyme was decreased by the deletion of nonconserved structural domains; however, when such deletions were made, there were severe losses of enzymatic activity. In vitro genetic selection was used to identify mutations that reactivate a virtually inactive *sunY* deletion mutant. A selected mutant with five substitution mutations scattered throughout the primary sequence showed greater catalytic activity than the original ribozyme under the selection conditions. The *sunY* ribozyme and its small selected variant can both catalyze template-directed oligonucleotide assembly. The small size and reduced secondary structure of the selected variant results in an enhancement, relative to that of the original ribozyme, of its rate of self-copying. This engineered ribozyme is able to function effectively both as a catalyst and as a template in self-copying reactions.

The idea of an RNA polymerase composed of RNA is central to current theories of the origin of life, since such a molecule could replicate autocatalytically. Such a self-replicating RNA molecule is commonly referred to as an RNA replicase. Because of the similarity between the chemistry catalyzed by group I introns (phosphodiester exchange reactions) and modern-day polymerases (phosphoanhydride-phosphodiester exchange reactions), we are attempting to use this class of ribozymes as a starting point from which to engineer an RNA replicase.

The authors are in the Department of Molecular Biology, Massachusetts General Hospital, Boston, Massachusetts 02114.

Previous studies (*1, 2*) have demonstrated that the *Tetrahymena* and *sunY* ribozymes can catalyze the ligation of oligonucleotides on exogenous templates. However, an RNA replicase would have to function efficiently as both a catalyst and a template. Conflicting requirements constrain the evolution (or design) of an RNA molecule that must play two such different roles. Maximal enzyme activity would presumably be enhanced by a strong secondary and tertiary structure, so that the three-dimensional structure required for substrate binding and catalysis will form. In contrast, elongation of the growing chain would presumably be enhanced on an unstructured (unfolded) template, so that template structure would not interfere with substrate binding. It appears that an RNA replicase must exist in a delicate balance between the folded state necessary for catalysis, and the unfolded state necessary for template activity. Furthermore, the transition between the folded and unfolded states should not be highly cooperative, so that both states can coexist over a broad range of conditions.

It was necessary to determine whether the enzymatic and template activities were mutually exclusive. Ribozymes such as the *Tetrahymena* and *sunY* introns are efficient catalysts, but their degree of structure would be likely to impede the synthesis of a complementary RNA. In contrast, small ribozyme derivatives with minimal overall structure, such as deletion derivatives generated from *sunY* (*3*), while seemingly better suited to function as templates, have thus far appeared to be poor catalysts. We have therefore applied the technique of iterative in vitro selection to the task of isolating a small but highly active ribozyme variant that can function efficiently as a template.

In vitro selection of catalytically active variants. The *sunY* intron from bacteriophage T4 is 245 nucleotides (nt) in length (without the open reading frame) and is one of the smallest known self-splicing introns (*4*). Previous efforts to further decrease the size of this intron included the removal of phylogenetically nonconserved domains, because these were unlikely to be essential to ribozyme function. While stem loops P9.1 and P9.2 (*5*) of *sunY* could be eliminated from the ribozyme with only minor losses in activity (the resulting 180-nt molecule was subsequently referred to as the "original" ribozyme, Fig. 1A) (*3, 6*),